The Canadian Mineralogist
Vol. 32, pp. 257-270 (1994)

STRUCTURAL VARIATIONS IN CHRYSOTILE ASBESTOS FIBERS REVEALED BY SYNCHROTRON X-RAY DIFFRACTION AND HIGH-RESOLUTION TRANSMISSION ELECTRON MICROSCOPY

BARBARA A. CRESSEY

Department of Geology, University of Southampton, Southampton, SO9 5NH, U.K.

GORDON CRESSEY

Department of Mineralogy, Natural History Museum, London, SW7 5BD, U.K.

ROBERT J. CERNIK

SERC Daresbury Laboratory, Warrington, WA4 4AD, U.K.

Abstract

Four samples of chrysotile asbestos have been studied by synchrotron X-ray diffraction. One of these samples exhibits asymmetrical 00*l* diffraction profiles, and also shows characteristics of "Povlen-type" chrysotile in X-ray fiber photographs. The 00*l* peak asymmetry is interpreted as indicating the presence of two layer-spacings, one about 7.3 Å, in common with the other chrysotile samples, and one about 7.2 Å. TEM images of the chrysotile with two apparent layer-spacings show the presence of fibers with both curved and flat layers in a variety of disordered tubular structures having only approximate cylindrical symmetry. The flat layers in these fibers may have a smaller interlayer-spacing (7.2 Å) relative to the curved layer-spacing (7.3 Å) because of the possibility of increased hydrogen bonding between flat layers that are stacked in register with one another. In this sample, fibers with flat layers parallel to one direction only, joined at each end by curved layers are observed to occur commonly. Also present are fibers with polygonal-tube cores made up from flat layers, with outer layers that are curved in a more normal way. This type of structure appears to be the closest that has been observed to the alternative structural model proposed by Middleton & Whittaker (1976) for "Povlen-type" chrysotile. In the same specimen, cylindrical chrysotile fibers that possess 5-fold symmetry have been imaged, in which the layer stacking is apparently in register radially at 15 points around the circumference, arising from the *b*/3 repeat of the hydroxyl layer.

Keywords: chrysotile, "Povlen-type" chrysotile, transmission electron microscopy, hydrogen bonds, asymmetrical diffraction-peak.

Sommaire

Quatre échantillons de chrysotile ont fait l'objet d'une étude par diffraction X avec un synchrotron comme source du rayonnement. Dans un de ces échantillons, qui possède les traits de chrysotile de type "Povlen" dans des clichés de fibres, les profils de diffraction 00*l* sont asymétriques. L'asymétrie serait due à la présence de deux espacements distincts entre les feuillets, un d'environ 7.3 Å, en commun avec les autres échantillons de chrysotile, et l'autre d'environ 7.2 Å. Les images prises par microscopie électronique par transmission montrent la présence de fibres ayant à la fois des feuillets courbes et plats dans une variété de structures tubulaires désordonnées qui n'ont qu'approximativement la symétrie cylindrique. Nous pensons que les feuillets plats dans ces fibres pourraient avoir un espacement inter-feuillet plus petit (7.2 Å) que les feuillets courbes (7.3 Å) à cause de la possibilité accrue de liaisons hydrogène entre les feuillets plats, empilés en registre les uns sur les autres. Dans cet échantillon, les fibres ayant les feuillets plats parallèles à une seule direction et joints aux deux bouts par des couches courbes sont très répandus. Sont aussi présents des fibres ayant un centre tubulaire polygonal à feuillets plats, avec des couches externes courbes de la façon plus courante. Ce type de structure semble se rapprocher le plus du modèle structural alternatif proposé par Middleton et Whittaker en 1976 pour expliquer le chrysotile de type "Povlen". Dans le même échantillon, des fibres cylindriques de chrysotile possédant un axe de symétrie 5 ont été photographiés dans lesquels l'empilement des couches serait en registre de façon radiaire à 15 points repères autour de la circonférence, conséquence de la période *b*/3 de la couche des groupes hydroxyles.

(Traduit par la Rédaction)

Mots-clés: chrysotile, chrysotile de type "Povlen", microscopie électronique par transmission, liaison hydrogène, pic de diffraction asymétrique.

INTRODUCTION

The cylindrical structure of chrysotile was first established by X-ray diffraction (Whittaker 1951, 1952, 1953, 1954, 1955a, b, c, d, 1956a, b, c, 1957). The tubular morphology of chrysotile was imaged by transmission electron microscopy (TEM) by various workers in the 1940s and 1950s, but clear confirmation that the tubular morphology is formed by a cylindrical lattice was provided by high-resolution TEM (Yada 1967, 1971). In his micrographs, the 7.3 Å (002) lattice fringes show that the sheets are curved as single or multiple spirals or as concentric cylinders. [The fringes corresponding to individual layers index as (002) because a two-layer cell ($c \approx 14.6$ Å) is usually used for clinochrysotile]. Radial 4.5 Å (020) fringes also were resolved; they are generally not straight but zig-zag in direction, as additional unit cells are incorporated around the circumference with increasing radius of the curved layers. Some of the micrographs also show some unusual growth-habits, with irregularly shaped fibers that seem to have grown in stages.

X-ray and electron diffraction patterns produced by splintery or lath-like varieties of chrysotile, commonly known as "Povlen-type" chrysotile, exhibit differences from the patterns produced by fibers of "normal" (silky) chrysotile (Eckhardt 1956, Zussman *et al.* 1957, Krstanovic & Pavlovic 1964, 1967). These patterns show a series of sharp *hkl* reflections on *h* odd layer lines instead of, or superimposed on, the *hk0* reflections with diffuse tails characteristic of the cylindrical wrapping of the structural layers in chrysotile. Middleton & Whittaker (1976) studied diffraction patterns produced by "Povlen-type" chrysotile in detail and concluded that the extra reflections resulted from a polygonal tubular structure, possibly with a core of normal, cylindrical chrysotile. An alternative arrangement of a polygonal core surrounded by cylindrical material also was proposed, but considered less likely to occur.

By using transmission electron microscopy, Cressey & Zussman (1976) observed fibers of polygonal serpentine of the kind postulated by Middleton & Whittaker. These polygonal fibers are composed of sectors of flat layers arranged to form polygonal prisms, either with or without a core of cylindrical chrysotile. All the polygonal fibers observed in cross-section using TEM have unusually large fiber diameters (up to 2000 Å) compared with normal chrysotile (generally 200 – 500 Å in diameter). "Povlen-type" diffraction effects also have been observed in single chrysotile fibers of "normal diameter" (up to 200 Å) seen longitudinally in the TEM (Middleton 1974), but until now cross-sections of normal-diameter "Povlen-type" fibers have never been observed. This may be because of the difficulties involved in obtaining thin, electron-transparent cross-sections of fibers by ion-beam thinning or other methods. More examples of similar polygonal fibers, and more complex structures with flat layers stacked in sectors, have been observed in subsequent TEM studies (Cressey 1979, Wei & Shaoying 1984, Mellini 1986, Yada & Wei 1987, Mitchell & Putnis 1988). Other, irregular structures involving curled layers passing laterally into flat layers have been recorded, *e.g.*, by Veblen & Buseck (1979) and Cressey & Hutchison (1984).

In this study, we show how modern high-resolution diffraction and imaging techniques (synchrotron X-ray diffraction and transmission electron microscopy) have provided new evidence on the nature of curved-layer and flat-layer structures in fibrous serpentines.

EXPERIMENTAL

We have investigated four samples of chrysotile asbestos from the collection of the Natural History Museum (Table 1) by X-ray diffraction using the Synchrotron Radiation Source (SRS) at the SERC Daresbury Laboratory, Warrington, U.K. These samples all consist of bundles of fibers up to 4 cm long which, in hand specimen, appear similar to many other (silky) chrysotile fibers, except that specimen BM1929,1974 is more splintery than most.

Synchrotron X-radiation is tuneable to a chosen wavelength and is delivered as a monochromatic, high-intensity, well-collimated, near-parallel beam, and thus instrumental peak broadening is minimized. Consequently, although chrysotile specimens produce peaks that are broadened because of the fine size of the fibrils (generally about 150 Å in diameter), resolution of the diffraction pattern is sufficiently good to enable observation of subtle structural variations in the diffraction profiles.

Bundles of asbestiform chrysotile fibers 20–30 mm long and about 0.5 mm in diameter were mounted horizontally on the axis of the goniometer of Station 9.1 of the SRS (Cernik & Bushnell-Wye 1991). With a count time of 1 second per step and a step size of 0.01° 2θ, diffraction data were recorded in Debye–Scherrer geometry from the stationary bundles of fibers. In this orientation of the cylindrical lattice, only 00*l* and 0*k*0 reflections are observed. Thus recorded, the X-ray diffraction pattern of one of the chrysotile specimens (BM1929,1974) shows a marked

TABLE 1. SAMPLES OF CHRYSOTILE STUDIED

BM1929,1974	Nil Desperandum mine, Zvishavane, Zimbabwe
BM1924,429	Dures' mine, Zvishavane, Zimbabwe
BM1929,250	Sherlock, Western Australia
BM1974,118	Cassiar, British Columbia

asymmetry of 00*l* peaks. To investigate further the significance of this unusual asymmetry in the peak, we have examined this specimen by high-resolution TEM. Samples were vacuum-impregnated with epoxy resin, and then cross-sections of these fiber bundles were cut and prepared for TEM by ion-beam thinning. Thinned samples were examined in a JEOL JEM 2000FX TEM, operating at an accelerating voltage of 200 kV.

X-Ray Diffraction

The 004 diffraction profiles from the four samples of chrysotile recorded using synchrotron radiation are shown in Figure 1. Clearly, one of these samples (BM1929,1974) shows distinct asymmetry of the 004 peak. Analysis of this profile, using a peak deconvolution procedure, suggests that two layer-spacings (7.31 Å and 7.21 Å) may be present. Subsequently, 0012 and 0016 profiles also were recorded; these show the same asymmetry with better resolution. This asymmetry of 00*l* peaks was not observed in patterns from any of the other chrysotile samples. In addition, a conventional X-ray photograph (recorded on film in a cylindrical camera using Cu$K\alpha$ radiation) of the chrysotile sample with two apparent layer-spacings shows characteristics of "Povlen-type" chrysotile, *i.e.*, additional sharp reflections appear superimposed on the diffuse tail of the 130 reflection. The other samples with single 00*l* peaks in their synchrotron X-ray diffraction patterns (corresponding to a layer-spacing of approximately 7.3 Å) have fiber photographs typical of normal chrysotile.

Figure 2 shows the asymmetrical diffraction profiles, peak profile fits and their residuals for the 004, 0012 and 0016 reflections, recorded from chrysotile BM1929,1974 using synchrotron radiation. A pseudo-Voigt function was used to model the peaks. Clearly, two peaks are required to fit the main peak and the shoulder region on the high-angle side, and these are centered about values that yield 7.31 Å and 7.21 Å for the layer-spacing d_{002}.

The profile fitting in Figure 2 was constrained by allowing only two peaks to contribute to the fit; this provides a simple interpretation in terms of two distinct layer-spacings. However, the real situation may be more complex, as variations in layer-spacings

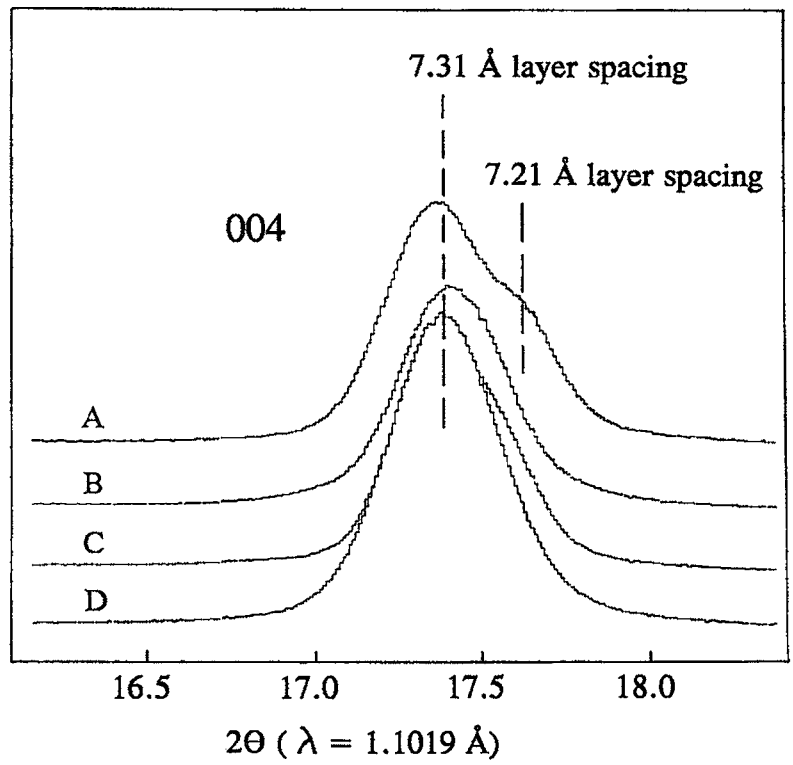

FIG. 1. Profiles of the 004 X-ray diffraction peak recorded from stationary samples of chrysotile fibers using synchrotron radiation. (A) BM1929,1974; (B) BM1929,429; (C) BM1974,118; (D) BM1929,250.

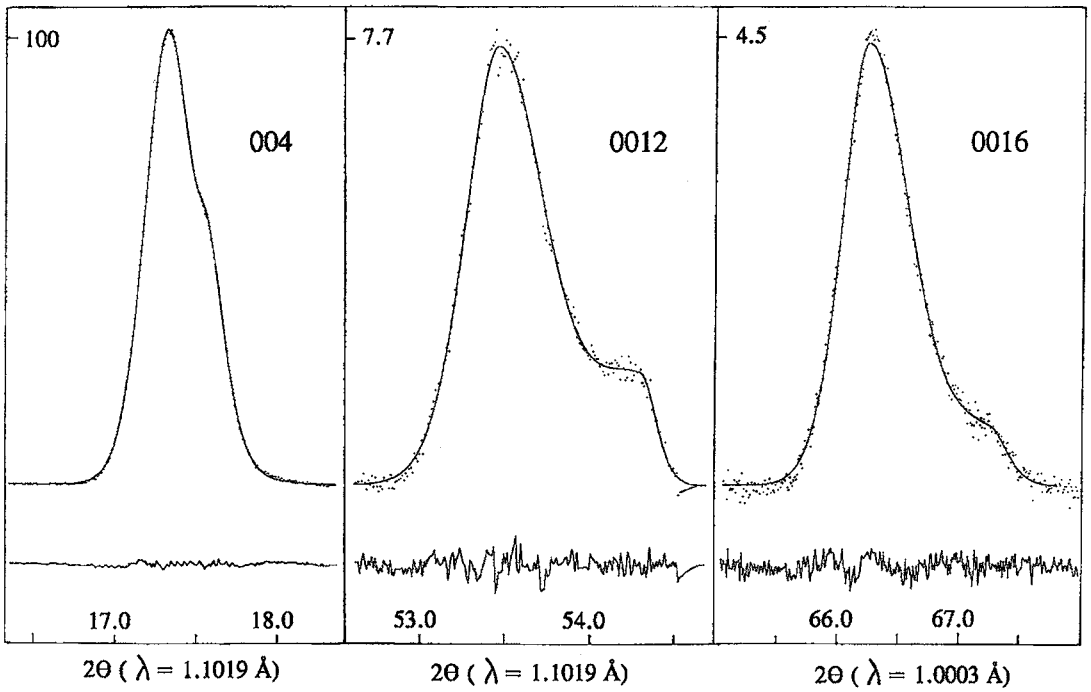

FIG. 2. Synchrotron X-ray diffraction profiles recorded from chrysotile BM1929,1974, together with profile fits (solid lines) and their residuals. In each case, two peaks have been used to fit the main peak and the shoulder. Note the relative decrease in the peak-height intensity of the shoulder with the increasing order of reflection. Intensities relative to the 004 peak are indicated on the vertical scale.

could occur, depending on the exact structure of the serpentine. Therefore, we also have performed fits with up to twelve peaks with unconstrained widths. By fitting with multiple peaks, it is apparent that the fine structure of the profiles can be modeled in more detail, suggesting that it may be appropriate to model these profiles with peaks that extend over a range of *d*-values corresponding to layer-spacings between 7.2 Å and 7.4 Å. It is also apparent that a greater spread of *d*-values contributes to the shoulder region than to the main peak. Modelling with multiple peaks still awaits quantitative analysis of peak positions and their widths, and further work on this is in progress.

However, a qualitative assessment of relative peak-widths can be made. It is evident that the relative peak-height of the shoulder component (representing the 7.21 Å layer-spacing) decreases almost linearly with $1/d$, and this reduction in peak height is likely to be due to peak broadening. Both peak components (7.31 Å and 7.21 Å) in the profile are broad, owing to the small size of the crystallites, but size-broadening is independent of the order of a reflection. However, peak broadening that arises from microstrain does depend on the order of a reflection, with peak breadth increasing as $1/d$ increases. This has been expressed by Langford *et al.* (1988) as $\beta = 4\tilde{e}/2d$, where β is the integral breadth, and $\tilde{e}$ denotes the microstrain. We therefore draw the conclusion that the serpentine structure with the smaller layer-spacing (7.21 Å) is significantly more strained.

As this chrysotile specimen is known to possess "Povlen-type" characteristics, it is likely that curved and flat layer structures are present (Middleton & Whittaker 1976, Cressey & Zussman 1976). The observed strain-broadening is consistent with the hypothesis that the structure of flat-layer serpentine is more strained than that of a curved-layer structure. In chrysotile, structural curvature enables partial compensation for the misfit between the sheets of octahedra and tetrahedra. Presumably, no such compensation occurs in flat-layer serpentine, unless substantial Al^{3+} and Fe^{3+} substitutions are present in the octahedrally and tetrahedrally coordinated sites. Energy-dispersion X-ray analysis of chrysotile BM1929,1974 in the SEM indicates the presence of only 1.5 wt% Fe and negligible Al. Structure refinements by Mellini (1982) and by Mellini & Zanazzi (1987) show that in lizardite (flat layers) the layer of tetrahedra is distorted to ditrigonal symmetry by rotation of tetrahedra to facilitate increased interlayer hydrogen bonding, even though an undistorted hexagonal arrangement of the layer of tetrahedra would be

more likely to reduce the intralayer misfit strain with the layer of octahedra. Chisholm (1992) has discussed the effects of intralayer and interlayer strain on the total strain associated with curved and flat layers in serpentine; from this assessment of strain, it can be appreciated that unless the fiber radius of chrysotile is either very small or very large, a curved structure is likely to possess less total strain than a flat-layer structure. There is, however, no clear indication in published cell parameters that samples of lizardite generally have smaller interlayer spacings than samples of chrysotile.

Electron Microscopy

Having seen features of "Povlen-type" chrysotile in single-crystal-type diffraction patterns from specimen number BM1929,1974, and evidence of both 7.31 Å and the unexpected 7.21 Å layer-spacings in the synchrotron XRD patterns, we have sought explanations for these features by high-resolution TEM. Our TEM observations of cross-sections of these fibers reveal tubes made up of curved and flat layers in disordered cylindrical structures, with only approximate rotational symmetry. We have not, however, found any large, polygonal fibers with clearly defined boundaries between sectors of flat plates, such as those seen previously in specimens of "Povlen-type" chrysotile.

Fibers that most closely resemble the "Povlen-type" chrysotile images previously published have cores of flat or gently curving layers. Curved sheets lack smooth, continuous cylindrical curvature but are arranged with discontinuously curved sections which, like the flat sheets, form approximately polygonal tubular cores. Examples are shown in Figure 3. The lattice fringes are, unfortunately, a little faint because

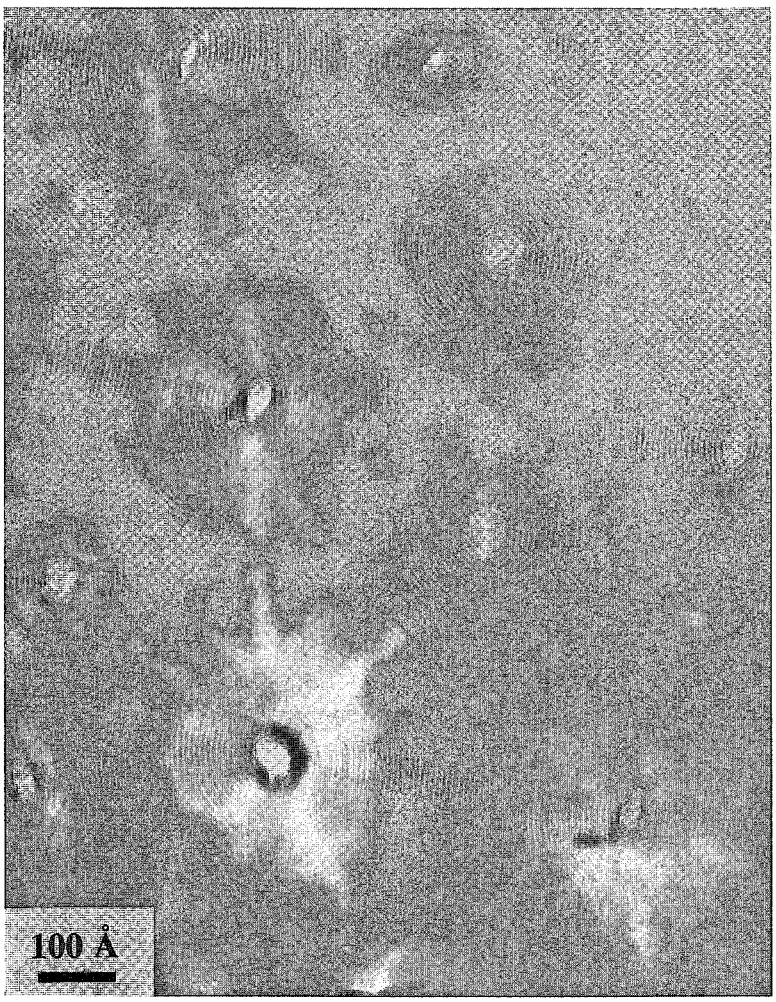

FIG. 3. TEM image of chrysotile BM1929,1974 with the beam parallel to the fiber axes, showing (002) lattice fringes. Note that several fibers have polygonal cores made up of flat layers, with outer layers that are more smoothly curved.

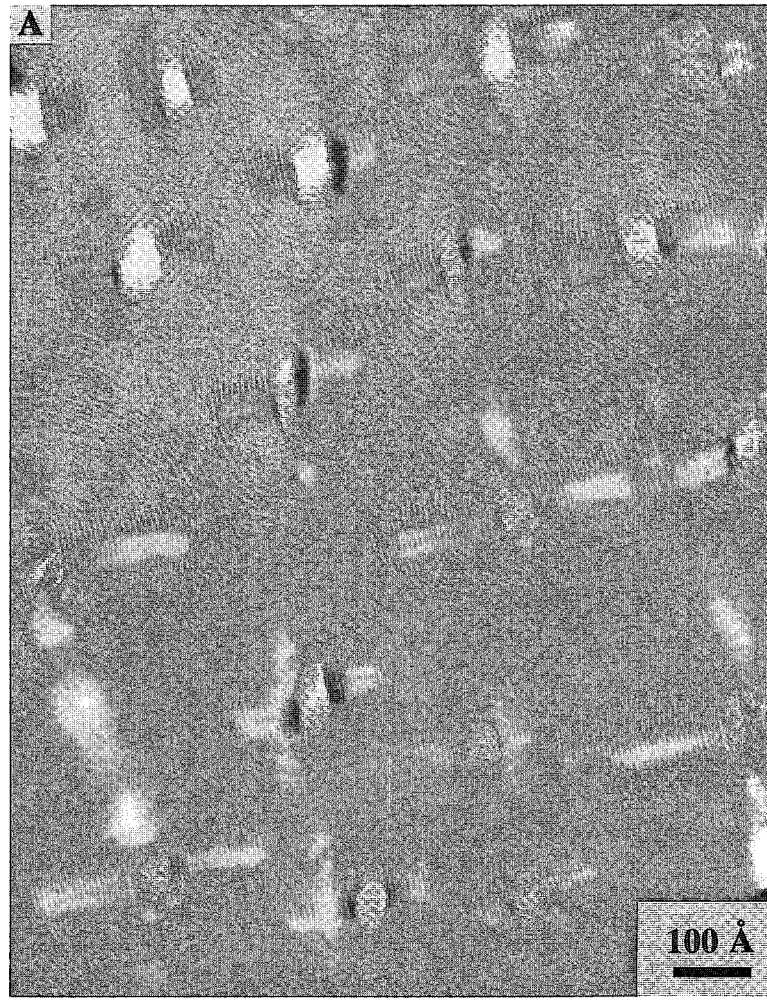

FIG. 4. Fiber sections recorded with the beam nearly parallel to the fiber axes. (A). These fibers have elongate cross-sections with straight (002) lattice fringes parallel to the elongation. (020) fringes are visible in curved sections of some fibers. (B). A fiber from (A) showing (002) and (020) fringes in opposite quadrants, both parallel to the plane containing the fiber axis and the beam. (C). A fiber from (A) showing (002) and (020) fringes that are not in exactly opposite quadrants, and the two fringe sets are not parallel to one another.

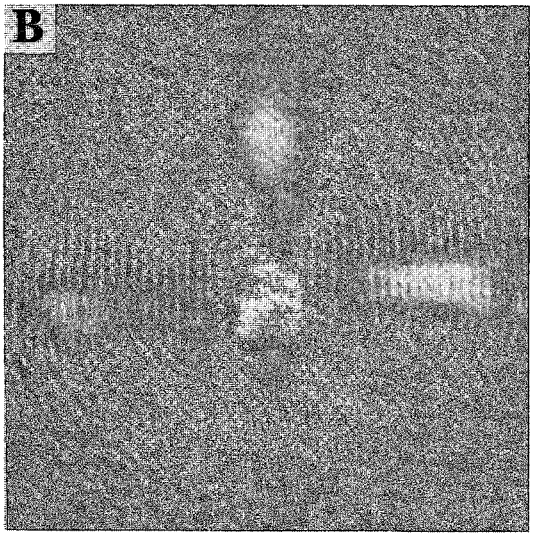

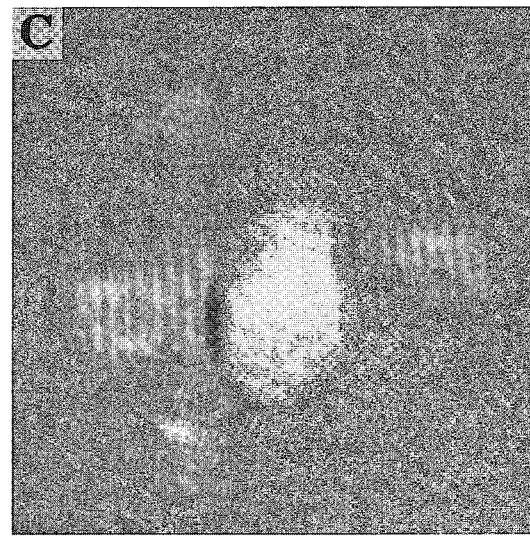

these fibers are in a very thin area of the specimen. Ion-beam thinning always produces a damaged, amorphous surface-layer. Adjacent to the edges of the holes produced by ion-beam thinning, the very thin parts of the specimen will therefore consist almost entirely of amorphous material. The outer layers of the fibers in Figure 3 are particularly indistinct because they have largely become amorphous, either during ion-beam thinning or during exposure to the electron beam. However, the outer layers, where visible, appear to be curved in a more normal way. These structures seem to be the closest that have been observed to the alternative model of the structure proposed by Middleton & Whittaker (1976) for "Povlen-type" chrysotile. We have found them occurring only very infrequently in the electron-transparent parts of this specimen.

We have, however, observed another structure involving flat and curved sheets in a fibrous habit in this specimen. In the thinned areas examined, it occurs with fairly high frequency. Fibers of this type consist of flat layers parallel to one direction only, joined coherently at each end by curved layers, resembling the appearance of an oval running track. A typical area containing such elongate cross-sections of fibers is shown in Figure 4. It is not possible to account for such elongation by assuming that the fiber axis is inclined to the electron beam; a tilt of 60° would be necessary to produce a ratio of minor to major axis of 1:2, as is observed here. In any case, such tilt would extinguish the (002) fringes on the long sides and leave them on the curved ends, which is the opposite of what we observe.

In the area shown in Figure 4, (002) fringes (concentric or spiral) are generally less clear around the curved parts of fiber sections. The flat layers seem to suffer damage under the electron beam less quickly than the curved parts. Commonly, (020) fringes (from center to circumference) are visible in the curved sections instead. If there is a slight misalignment of the fiber axis with respect to the electron beam, then the (020) and (002) fringes would tend to persist in alternate quadrants, and both sets of fringes would be parallel to the plane containing the fiber axis and the beam. Generally, this appears to be the case in Figure 4 (*e.g.*, Fig. 4B), where the axes of elongation

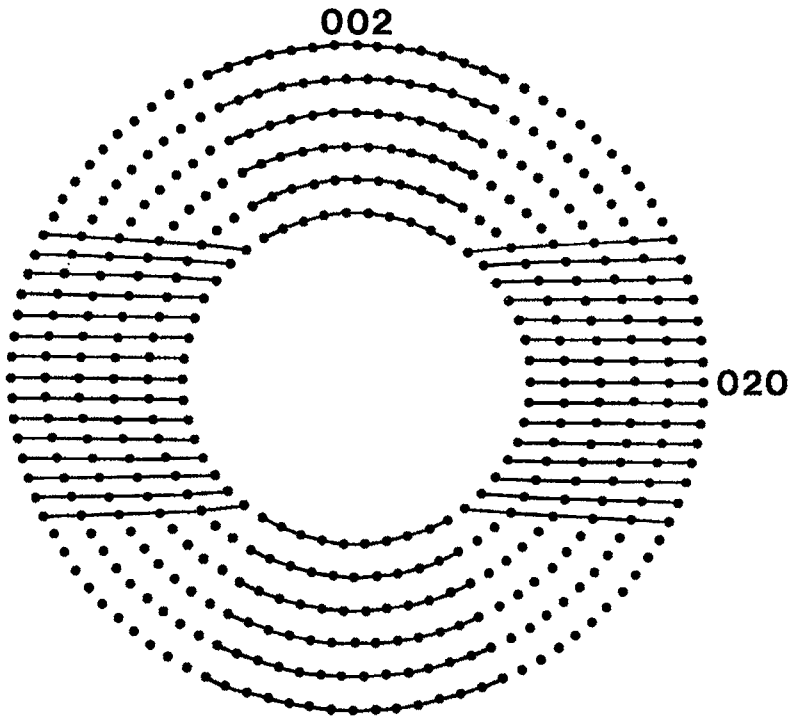

FIG. 5. A cylindrical array of lattice points (after Whittaker 1955b) joined in such a way as to represent the lattice fringes shown in Figure 4B. Note, however, that in Figure 4 the (002) fringes are mostly straight, not curved as here, because the fiber is oval in cross-section, not circular.

happen to be roughly parallel to the plane containing the fiber axes and the beam.

It should be noted that (020) fringes are not truly radial, or they would diverge from the center with additional unit cells added around the circumference as the radius of the curved layer increases, giving the zig-zag appearance shown by Yada (1971). In Figure 4, the (020) fringes are generally straight and equally spaced over considerable areas, to a fair degree of approximation, though there are some departures. Whittaker (1955b) used a mask for optical diffraction in which the dots lined up over considerable areas. In Figure 5, a section of Whittaker's cylindrical mask is reproduced, with lattice points joined up in such a way as to resemble the distribution of (020) and (002) fringes that we observe. In Figure 4, some sections (*e.g.*, Fig. 4C) show clear (020) and (002) fringes that are not strictly in alternate quadrants, and (020) fringes are not parallel to (002) fringes. This suggests that the position and orientation of the planes where the points of the circular (or distorted circular) lattice line up with each other need not be in alternate quadrants. It seems reasonable that they could easily be offset by up to 36° from the obvious positions, *i.e.*, the angle between the clear (002) and (020) fringes could be anything up to this angle, and not constant from center to circumference, as appears to be the case in some of the fiber sections shown here.

Not all fibers are elongate in cross-section with flat layers. Some are elongate but consist of curved sheets with variable radii of curvature, particularly in the core regions, and others are more nearly circular in section. Multilayer spirals also are found fairly commonly. A few examples are shown in Figure 6. Boundaries between fibers commonly are indistinct, with spaces between fibers filled by amorphous or

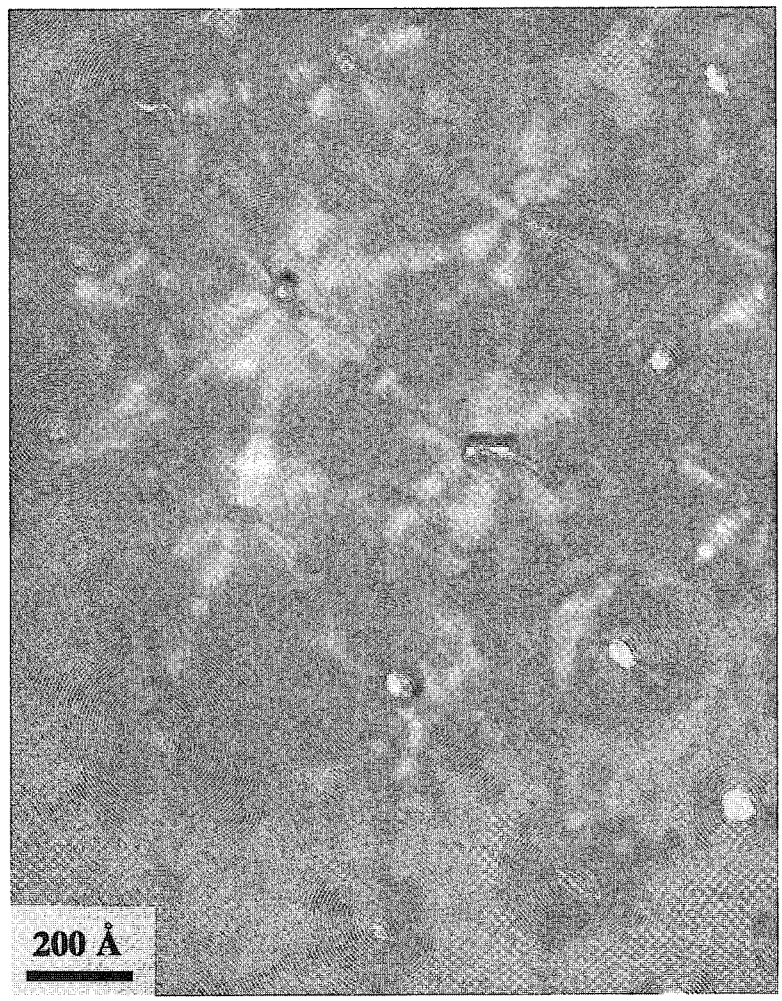

FIG. 6. Fiber sections exhibiting various growth irregularities, including variable radii of curvature and multi-layer spirals.

poorly crystalline material, or curved sheets. Central voids in fibers are commonly filled with similar material, and some fibers have very irregularly shaped but continuous sheets in the core regions, which may bridge the central holes. Whittaker (1957) suggested that such infilling would be likely, and would explain the observed measurements of density. It is not possible to know how much of the material with no apparent structure was originally amorphous and how much has become so because of damage in the electron beam or during specimen preparation.

In parts of the specimen that are thicker, a combination of strong diffraction-contrast and a degree of damage under the electron beam shows a pattern that indicates the existence of five-fold symmetry. This first demonstration of five-fold symmetry in a natural crystalline material has been reported elsewhere (Cressey & Whittaker 1993). Because this observation has implications concerning the nature of the interlayer bonding in this specimen, it is also described here.

Where fibers are exactly parallel to the beam, diffraction contrast makes them appear completely dark. With increased exposure to the electron beam, the dark contrast breaks into radial bands, with the diffraction contrast being lost from the outside edge first and extending toward the center with time. Figure 7 shows examples of this behavior. In this area, fibers are circular in section. Dark diffraction-contrast remains where (002) fringes are clearly visible and fades where the fringes disappear as these areas become amorphous under the beam. There are almost always 15 radial bands; the number 15 is significant. As pointed out by Whittaker (1954), $2\pi\ d_{002}$ is approximately equal to $5b$, so that if two successive layers are in step with one another somewhere, then they will be

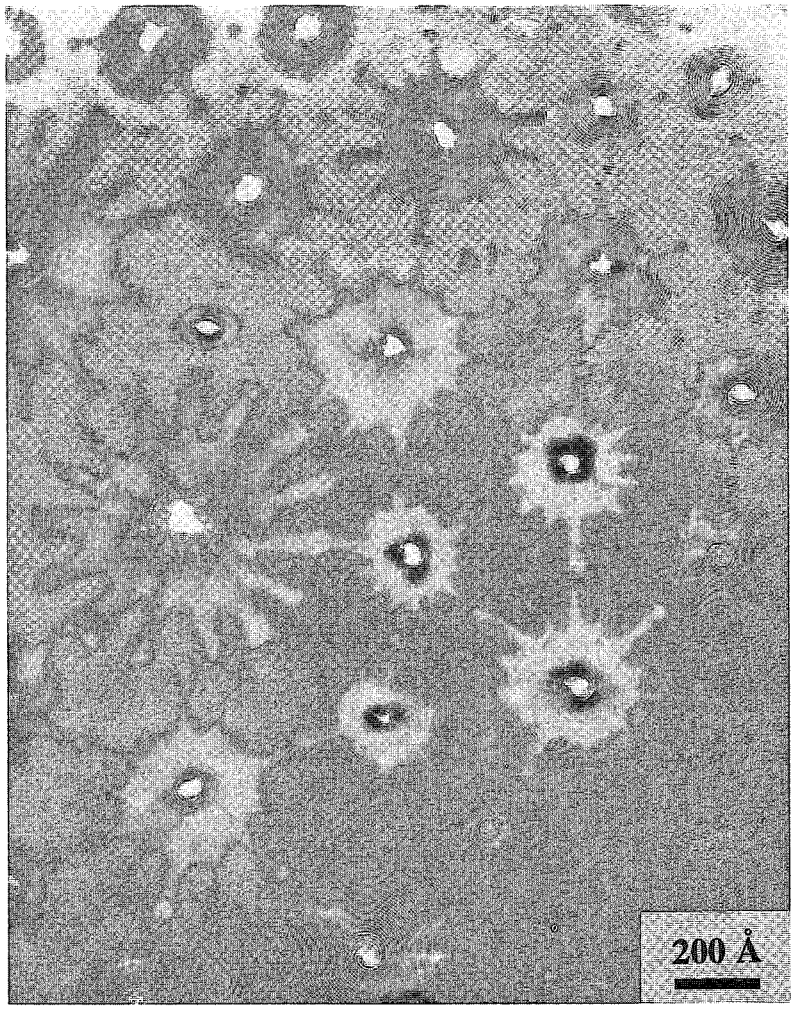

FIG. 7. Sections of fibers with their axes exactly parallel to the beam. Strong diffraction-contrast, which initially made the fiber sections appear completely dark, has broken into 15 radial bands after a period of exposure to the electron beam has caused some of the structure to become amorphous.

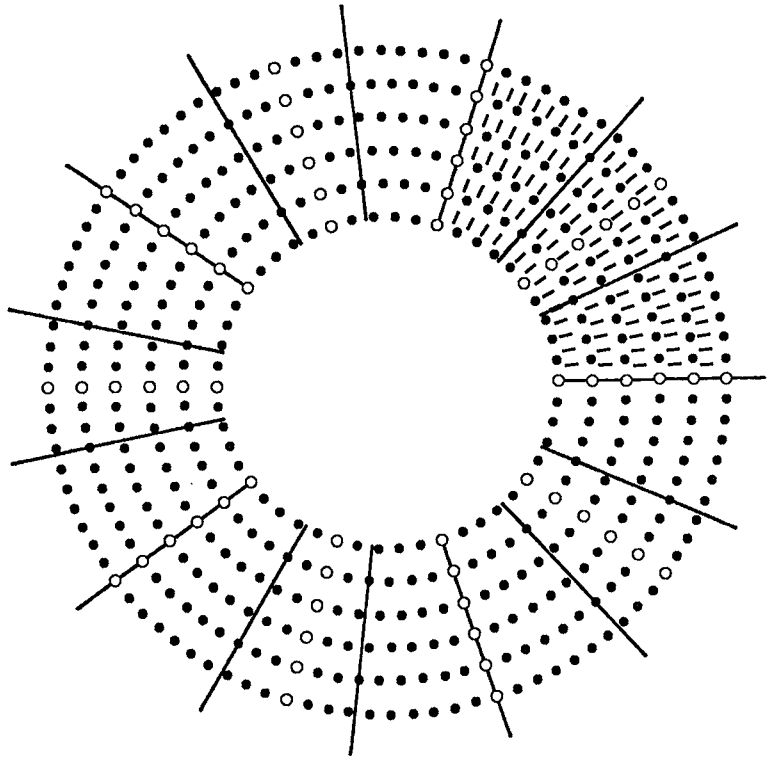

FIG. 8. A cylindrical array of lattice points (after Whittaker 1955b), representing a projection of the chrysotile lattice in cross-section. The points are separated circumferentially by *b*/2 to allow for the effect in projection of the centered unit-cell down *a*, and those marked with open circles are rows of points that exactly line up radially, ten times in projection. Note that alternate rows of open circles represent lattice points at height zero and *a*/2, so the overall symmetry is five-fold. Ticks with circumferential spacing of *b*/3, to represent the repeat of the hydroxyl side of the serpentine layer, are shown for successive serpentine layers in one of the five sectors. Solid lines represent the 15 radial positions (arising from the *b*/3 repeat of the hydroxyl groups) where local similarity of structure between the hydroxyl groups of one layer and the basal oxygen atoms of the next layer outward could allow hydrogen bonding to occur between successive layers.

in step five times around the circumference of the fiber. If all the layers are in step on a radial plane, then they are all in step five times. In Figure 8, we reproduce Whittaker's mask, marking with open circles those lattice points that line up radially. On the mask, the lining-up occurs ten times around the circumference because the lattice points are separated by *b*/2 to allow for the effect of projection of the centered unit-cell down *a*. [This is, of course, why we always observe (020) fringes]. If the structure were more susceptible to decomposition under the electron beam where the layers are out of step, then one could produce an effect similar to that in Figure 7, but with only five spokes. However, the hydroxyl side of the serpentine layer has a repeat of only *b*/3, so there is local similarity of the arrangement of the basal atoms of oxygen of one layer with respect to hydroxyl groups of the next inward 15 times per circumference. These 15 positions are marked on the diagram in Figure 8. The areas between these 15 spokes, where layers are out of step and so hydrogen bonding between layers is not possible, could well produce 15 radial bands where decomposition under electron bombardment takes place more readily, as seen in Figure 7.

Chisholm (1992) has pointed out that polygonal serpentine almost always has 15 sectors (or, less commonly, 30), because minimal misfit occurs only for polygonal microstructures with 15 or 30 sectors,

depending on the exact cell dimensions of the flat layers. A close inspection of Figure 7 suggests that possibly, in some fiber cross-sections, the (002) layers are not smooth, continuous curves. In the bands where less decomposition has occurred (*i.e.*, those regions where successive layers are probably more nearly in step with one another), the layers may seem to be flatter. (Care must be taken not to mistake contrast reversals along a layer for discontinuities of curvature). Possibly, under the right geological conditions, fibers such as these could recrystallize to form large, well-developed polygonal fibers similar to those seen in previous TEM studies, with 15 sectors, as discussed by Chisholm. Such recrystallization would increase the extent to which sheets could be stacked in register with one another. For large-radius fibers, this would be a much more stable arrangement, as pointed out by Chisholm (1992).

The specimen in which Cressey & Zussman (1976) originally found a high proportion of polygonal fibers comes from a serpentinite that has undergone prograde metamorphism after the initial serpentinization. The polygonal fiber shown in Cressey & Zussman (1976, Fig. 4) appears to have overgrown earlier-formed cylindrical fibers of chrysotile. A high-resolution micrograph of another polygonal fiber from the same specimen, shown in Figure 9, shows that layers are mostly coherent across sector boundaries. This micrograph also shows that in the cylindrical core, the sheets seem to be somewhat disordered in comparison with the outer, flat layers. These observations are in accord with our proposed mechanism for the formation of polygonal fibers by recrystallization, involving an adjustment of the interlayer stacking from a disordered to a more ordered arrangement. The fiber section is not a complete polygon, and in the missing parts where the sheets are not constrained, they tend to curl. These curved sections have small radii of curvature, similar to the normal, cylindrical fibers.

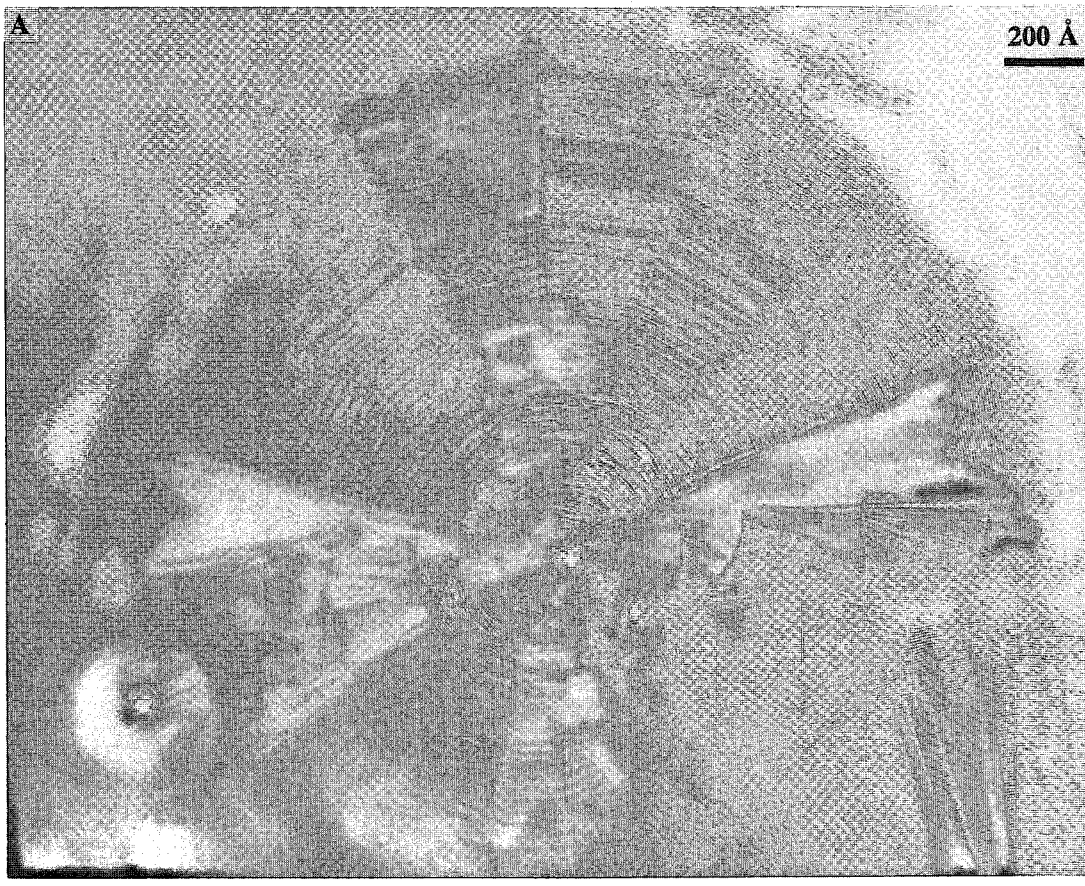

Figure 9A

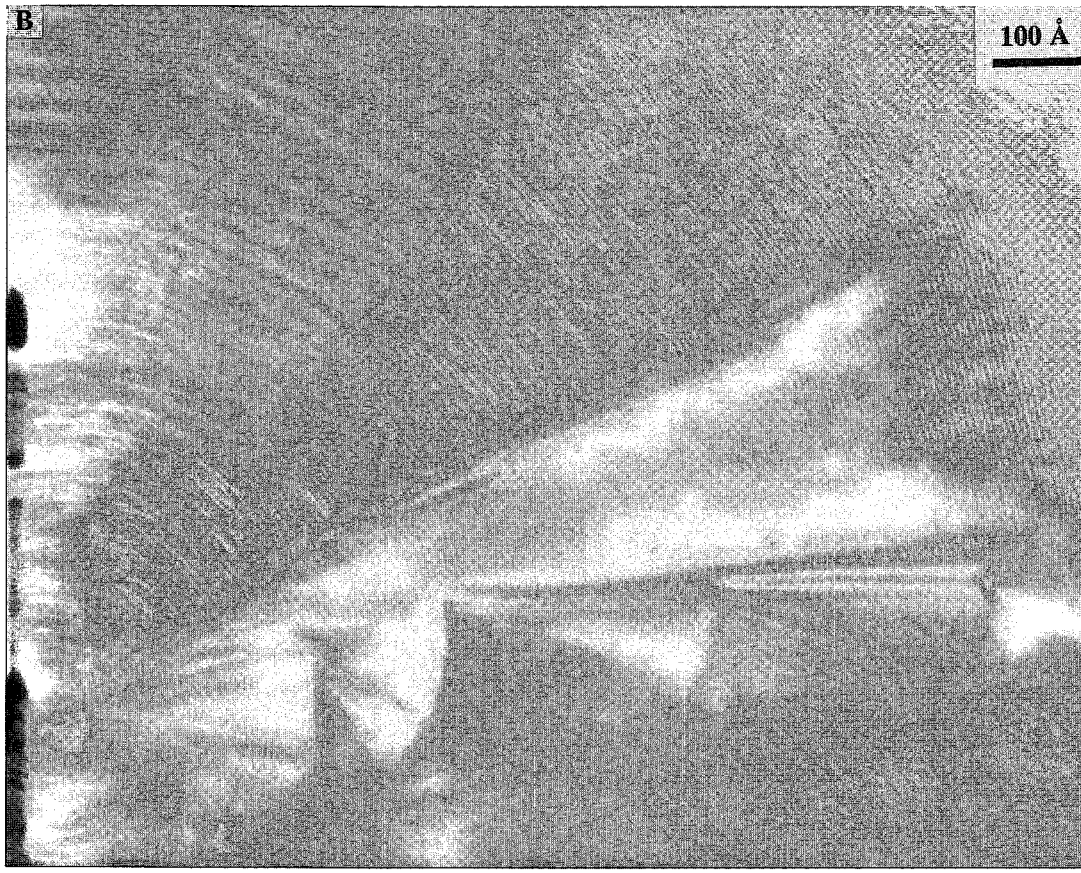

FIG. 9. High-resolution TEM image of a polygonal serpentine fiber, specimen 18501 (see Cressey & Zussman 1976). (A) The whole fiber section and (B) enlarged detail from part of (A), showing flat layers passing coherently across sector boundaries and continuing laterally into curved sheets. Note also the degree of disorder between layers in curved sheets near the fiber center.

Where fibers are slightly tilted with respect to the electron beam, then the (020) and (002) fringes tend to persist in alternate quadrants, as described above. Such a degree of misalignment gives rise to four radial dark bands of diffraction contrast, replacing the complete darkness or many (generally 15) bands seen where alignment of the fiber axis with the beam is more perfect. With slightly more misalignment, or greater damage under the electron beam, or both, the (020) fringes tend to disappear, leaving only the (002) fringes and one pair of dark diffraction-contrast bands at 180°. This pattern of diffraction-contrast behavior with tilt was noted by Cressey & Zussman (1976), though at the time there was no evidence to explain why it happens.

DISCUSSION

From the split (00*l*) reflections observed in the synchrotron diffraction profile of specimen BM1929,1974, two layer-spacings appear to be present. One is 7.31 Å, about the value normally found for chrysotile, and the other is about 7.21 Å. Electron microscopy suggests that the most obvious difference between this and other chrysotile specimens is the presence of substantial numbers of fibers with flat layers in this specimen. It appears that the flat layers in many of the fibers have a smaller interlayer-spacing because of the hydrogen bonding developed between flat layers that are stacked in register with one another. In cylindrical layers of chrysotile, micrographs such as

that shown by Yada (1971, Fig. 14) illustrate fibers in which layers are stacked completely randomly, out of register with one another. In the cylindrical fibers shown in this paper, the layer stacking is apparently in register at fifteen points around the circumference, but at all other positions the layers must be stacked out of register with one another. In cylindrical fibers, therefore, hydrogen bonding between layers is not generally possible. Published values for the layer-spacings of chrysotile and lizardite, the flat-layer variety of serpentine, suggest that there is a range of values from a little above 7.2 Å [*e.g.*, 7.233 Å for a lizardite reported by Mellini (1982)] to over 7.3 Å. However, there is no clear pattern of lizardite tending toward the lower value and chrysotile the higher. Lizardite commonly has a significant degree of disorder in its structure, and commonly contains more Al and Fe than chrysotile.

When we study ion-thinned specimens by TEM, it is inevitable that we can only image a tiny proportion of the material in any specimen. This is especially true for sections of asbestos fibers embedded in resin; the vast majority of the areas thinned to electron transparency consist of the resin. Therefore, we can never be sure of the extent to which our TEM observations are representative of the whole specimen. X-ray diffraction, however, gives us information averaged over a much larger volume. We cannot say with confidence that in specimen BM1929,1974, the proportion of flat layers relative to curved layers seen in the TEM corresponds with the ratio of 7.21 Å to 7.31 Å layer-spacing detected by X-ray diffraction, but the comparison seems reasonable, as far as we can judge. It would be interesting to carry out synchrotron X-ray diffraction experiments on fiber bundles consisting entirely of well-formed polygonal serpentine if sufficiently large bundles of long, parallel fibers could be found.

In specimen BM1929,1974, the elongate-sectioned fibers tend to be aligned with the axes of elongation all in roughly the same direction. Possibly these fibers suffered directional pressure during growth, or later deformation while still in the host rock. The possibility of deformation during specimen preparation must be considered, but it seems more likely that such processes would cause brittle fracture rather than plastic deformation. We have seen no evidence of broken fibers.

Our findings show, yet again, that the serpentine group of minerals can form in numerous complex structural arrangements that may seem difficult to classify. Imaging by high-resolution TEM shows that, on a fine scale, the structures commonly consist of mixtures or intermediate forms. Layers commonly pass coherently from one structure type to another over a few unit cells. Nevertheless, all the observed variations can be described as consisting of components of the three known structure types: cylindrical chrysotile, flat-layer lizardite or alternating-wave antigorite. A single fiber may therefore consist of both chrysotile and lizardite. Transitions from one structure type to another occur as the best solution to the problems caused by interlayer and intralayer strain at the time of crystallization (or recrystallization) in response to the local physicochemical conditions affecting each group of atoms. Most serpentinites have been formed under disequilibrium conditions, so perhaps it should not seem surprising to find that so many composite or intermediate structures exist.

Acknowledgements

We thank Dr. Eric Whittaker and Prof. Jack Zussman for helpful comments on our observations, kindly sharing with us their considerable wisdom and experience of the serpentine minerals. The referees are also thanked for their comments and suggestions. Mr. Tony Wighton, Natural History Museum, is thanked for producing excellent-quality demountable polished thin sections of chrysotile. We acknowledge funding by a SERC grant to carry out the synchrotron X-ray diffraction experiments.

References

Cernik, R.J. & Bushnell-Wye, G. (1991): The use of Debye–Scherrer geometry for high resolution powder diffraction. *Mater. Sci. Forum* **79-82**, 455-462.

Chisholm, J.E. (1992): The number of sectors in polygonal serpentine. *Can. Mineral.* **30**, 355-365.

Cressey, B.A. (1979): Electron microscopy of serpentinite textures. *Can. Mineral.* **17**, 741-756.

_____ & Hutchison, J.L. (1984): Microstructure of antigorite revealed by high resolution electron microscopy. *Inst. Phys. Conf., Ser.* **68**, 409-412.

_____ & Whittaker, E.J.W. (1993): Five-fold symmetry in chrysotile asbestos revealed by transmission electron microscopy. *Mineral. Mag.* **57**, 729-732.

_____ & Zussman, J. (1976): Electron microscopic studies of serpentinites. *Can. Mineral.* **14**, 307-313.

Eckhardt, F.-J. (1956): Röntgenographische Untersuchungen am Schweizerit. *Neues Jahrb. Mineral. Monatsh.*, 32-43.

Krstanović, I. & Pavlović, S. (1964): X-ray study of chrysotile. *Am. Mineral.* **49**, 1769-1771.

_____ & _____ (1967): X-ray study of six-layer orthoserpentine. *Am. Mineral.* **52**, 871-876.

Langford, J.I., Delhez, R., de Keijser, T.H. & Mittemeijer, E.J. (1988): Profile analysis for microcrystalline properties by the Fourier and other methods. *Aust. J. Phys.* **41**, 173-187.

MELLINI, M. (1982): The crystal structure of lizardite 1T: hydrogen bonds and polytypism. *Am. Mineral.* **67**, 587-598.

_____ (1986): Chrysotile and polygonal serpentine from the Balangero serpentinite. *Mineral. Mag.* **50**, 301-305.

_____ & ZANAZZI, P.-F. (1987): Crystal structures of lizardite-*1T* and lizardite-*2H1* from Coli, Italy. *Am. Mineral.* **72**, 943-948.

MIDDLETON, A.P. (1974): *Crystallographic and Mineralogical Aspects of Serpentine.* D.Phil. thesis, Oxford Univ., Oxford, U.K.

_____ & WHITTAKER, E.J.W. (1976): The structure of Povlen-type chrysotile. *Can. Mineral.* **14**, 301-306.

MITCHELL, R.H. & PUTNIS, A. (1988): Polygonal serpentine in segregation-textured kimberlite. *Can. Mineral.* **26**, 991-997.

VEBLEN, D.R. & BUSECK, P.R. (1979): Serpentine minerals: intergrowths and new combination structures. *Science* **206**, 1398-1400.

WEI, L. & SHAOYING, J. (1984): The discovery of Povlen-type hydroxyl-chrysotile and its mineralogy. *Acta Mineral. Sinica* **2**, 111-116.

WHITTAKER, E.J.W. (1951): An orthorhombic variety of chrysotile. *Acta Crystallogr.* **4**, 187-188.

_____ (1952): The unit cell of chrysotile. *Acta Crystallogr.* **5**, 143-144.

_____ (1953): The structure of chrysotile. *Acta Crystallogr.* **6**, 747-748.

_____ (1954): The diffraction of X-rays by a cylindrical lattice. I. *Acta Crystallogr.* **7**, 827-832.

_____ (1955a): The diffraction of X-rays by a cylindrical lattice. II. *Acta Crystallogr.* **8**, 261-265.

_____ (1955b): The diffraction of X-rays by a cylindrical lattice. III. *Acta Crystallogr.* **8**, 265-271.

_____ (1955c): The diffraction of X-rays by a cylindrical lattice. IV. *Acta Crystallogr.* **8**, 726-729.

_____ (1955d): The classification of cylindrical lattices. *Acta Crystallogr.* **8**, 571-574.

_____ (1956a): The structure of chrysotile. II. Clinochrysotile. *Acta Crystallogr.* **9**, 855-862.

_____ (1956b): The structure of chrysotile. III. Orthochrysotile. *Acta Crystallogr.* **9**, 862-864.

_____ (1956c): The structure of chrysotile. IV. Parachrysotile. *Acta Crystallogr.* **9**, 865-867.

_____ (1957): The structure of chrysotile. V. Diffuse reflections and fibre texture. *Acta Crystallogr.* **10**, 149-156.

YADA, K. (1967): Study of chrysotile asbestos by a high resolution electron microscope. *Acta Crystallogr.* **23**, 704-707.

_____ (1971): Study of microstructure of chrysotile asbestos by high resolution electron microscopy. *Acta Crystallogr.* **A27**, 659-664.

_____ & WEI, L. (1987): Polygonal microstructures of Povlen chrysotile observed by high resolution electron microscopy. *Euroclay 87 (Sevilla, Spain), Abstr.*

ZUSSMAN, J., BRINDLEY, G.W. & COMER, J.J. (1957): Electron diffraction studies of serpentine minerals. *Am. Mineral.* **42**, 133-153.

Received April 7, 1993, revised manuscript accepted August 22, 1993.